WILEY VCH

Yunlong Zi, Hengyu Guo, Jie Wang, Chi Zhang,
Xiangyu Chen, and Qing Zhao

Triboelectric Nanogenerators

Technology, Applications, and Commercialization

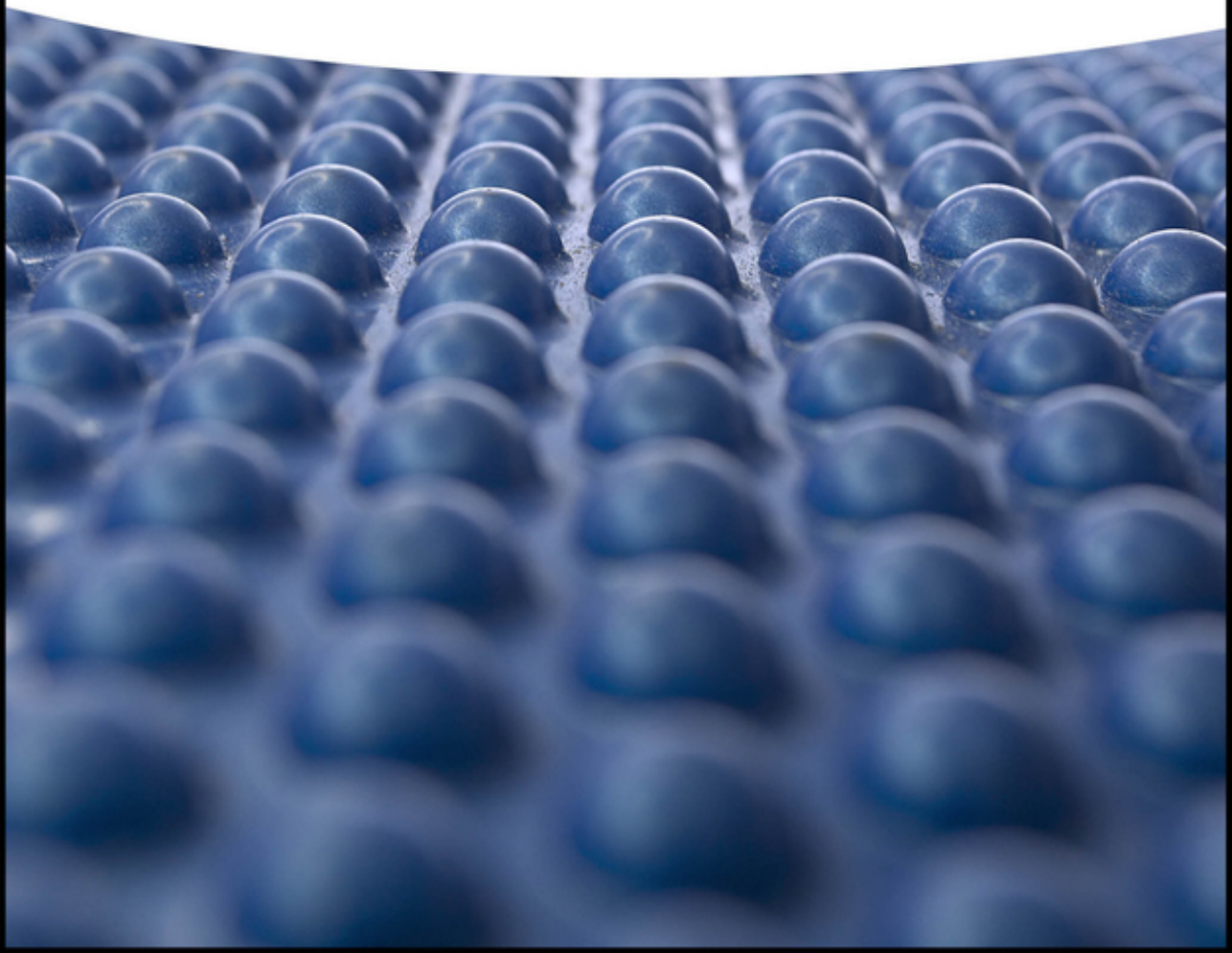

Triboelectric Nanogenerators

Triboelectric Nanogenerators

Technology, Applications, and Commercialization

Yunlong Zi, Hengyu Guo, Jie Wang, Chi Zhang, Xiangyu Chen, and Qing Zhao

WILEY VCH

Authors

Yunlong Zi
Hong Kong University of Science and Technology (Guangzhou)
Guangzhou, Guangdong
China

Hengyu Guo
Chongqing University
Chongqing
China

Jie Wang
Beijing Institute of Nanoenergy
Beijing
China

Chi Zhang
Beijing Institute of Nanoenergy
Beijing
China

Xiangyu Chen
Beijing Institute of Nanoenergy
Beijing
China

Qing Zhao
Chongqing University
Chongqing
China

Cover Image: © Carlos Barros/Getty Images

Library of Congress Card No.: applied for

British Library Cataloguing-in-Publication Data
A catalogue record for this book is available from the British Library.

Bibliographic information published by the Deutsche Nationalbibliothek
The Deutsche Nationalbibliothek lists this publication in the Deutsche Nationalbibliografie; detailed bibliographic data are available on the Internet at <http://dnb.d-nb.de>.

The manufacturer's authorized representative according to the EU General Product Safety Regulation is WILEY-VCH GmbH, Boschstr. 12, 69469 Weinheim, Germany, e-mail: Product_Safety@wiley.com.

Print ISBN: 978-3-527-35042-1
ePDF ISBN: 978-3-527-83788-5
ePub ISBN: 978-3-527-83789-2
oBook ISBN: 978-3-527-83790-8

Typesetting Straive, Chennai, India

Contents

Preface

Since its invention, triboelectric nanogenerator (TENG) has experienced development for over 10 years, like a big tree grown from a tiny seed. 10 years ago, we were still working on the basic modes, fundamental theories, evaluation standards, etc. Five years ago, we studied mechanisms and designs that can enhance the output performance of TENGs. Nowadays, TENG has become a well-recognized energy harvesting technology with output energy density of 10^5 J/m^3 level while the peak power density can achieve 15 MW/m^2, and scientists are working on TENG's applications in various scenarios. As recommended by authors, we believe the topics selected are important research topics in TENG, which may not only contribute to the development of science in TENG, but also promote the applications. The significance and the related questions of these chapters are stated below:

1) Chapters 1 and 2 state how the triboelectric charge was generated and discharged, which highlights the charge transfer flow in TENG. In the meanwhile, an issue worthy to discuss is how the energy conversion in TENG was completed at the beginning, and how a large portion of the electrostatic energy was wasted if they were not used in applications.
2) Chapter 3 regarding the standardization of TENG is touching a key question of TENG, that is how much energy can TENG provide? The provided standards are all related the output energy density of TENG, which is now around 10^5 J/m^3. As comparison, the lithium ion battery can achieve around 10^9 J/m^3, while the limit of the breakdown discharge of materials is around 10^8 J/m^3, which means we may still have some gaps to catch.
3) Chapters 4–8 discuss about different methods to promote and/or config the output performance of TENGs. The gas environment can impact the breakdown discharge limits as well as equivalent resistance of among triboelectric layers and electrodes. Liquid–solid interface may provide a way for triboelectric charge generation with little energy waste in friction. Electromechanical structures may provide means to excite the charge in circles until breakdown limit. DC-TENG provides a new design that can directly supply direct current output. The power-management and energy storage systems provide solutions to manage and store the generated power, which is also necessary in the system.

4) Chapters 9–12 outlook four new related research areas, which are all related to potential applications. Tribotronics utilizes TENG to serve as a gate voltage, which can be triggered by simply touching. Tribophotonics couples the triboelectricity as the power source and photonics as the wireless transmission means, targeting at self-powered wireless systems. Combined with artificial intelligence (AI), sensing systems based on TENG mechanisms will become more accurate, with advantages of high signal-to-noise ratio. High-voltage output from TENG, with thousands or even tens of thousands volts in voltage, may be a new application area that is promising to trigger breakdown discharge, electrospray, field emission, etc.

In light of the four parts as stated above, we can see that TENG is experiencing a rapid development in the past five years. Compared with the book *Triboelectric Nanogenerators* published in 2016 by Springer, the contents of this book cover more in-depth mechanism studies, discuss more methods to promote/regulate the output performance, and expands more applications with new research directions proposed. Hopefully with this new book, readers can understand the progress in this exciting field, and facilitate mutual communications among scientists, engineers, students, and public, which may end up with better utilization of TENG technology to serve the people's life.

Introduction of Triboelectric Nanogenerator

I.1 What is a Triboelectric Nanogenerator (TENG)?

To meet the rapidly increased energy demands of the Internet of Things (IoT) and modern smart cities, a new type of energy harvesting technology, nanogenerator, has been invented to provide sustainable power source by collecting energy from the ambient environment. In them, the triboelectric nanogenerator (TENG), which is based on the coupling of triboelectrification and electrostatic induction effects, is focused in recent years [1–6]. This emerging technology was predicted to play a critical role in harvesting low-frequency energy such as body motion energy and ocean-wave energy [7–9]. Due to its advantages of lightweight, low cost, and high efficiency, plenty of research has demonstrated the great potential of TENGs on numerous applications [10–13].

The term "nanogenerator" is defined as an emerging type of technology that can convert small-scale mechanical and thermal energy into electricity. Different from traditional generators, nanogenerator usually utilizes Maxwell's displacement current initiated by the static charges, which were generated by triboelectric, piezoelectric, and pyroelectric effects, to drive effective energy conversion [14, 15]. TENG is the major type of nanogenerator which utilizes the charge generated in triboelectric effect, which is also the most powerful energy harvester in nanogenerators.

I.2 First-Principle Theoretical Model

Traditionally, it is believed that TENG is operated based coupling effects of triboelectrification and electrostatic induction. Triboelectrification (triboelectric effect) describes the origin of the static charges, while electrostatic induction explains the power generation. However, further theories from fundamental physics are still required to understand the operation of TENG.

Triboelectric Nanogenerators: Technology, Applications, and Commercialization, First Edition.
Yunlong Zi, Hengyu Guo, Jie Wang, Chi Zhang, Xiangyu Chen, and Qing Zhao.

Wang demonstrated the first-principle theoretical models from Maxwell's displacement current [14, 15]. Maxwell's equations are shown below:

$$\begin{aligned} &\nabla \cdot \boldsymbol{D} = \rho \\ &\nabla \cdot \boldsymbol{B} = 0 \\ &\nabla \times \boldsymbol{E} = -\frac{\partial \boldsymbol{B}}{\partial t} \\ &\nabla \times \boldsymbol{H} = \boldsymbol{J} + \frac{\partial \boldsymbol{D}}{\partial t} \end{aligned} \tag{I.1}$$

Here, $\boldsymbol{D} = \varepsilon \boldsymbol{E}$ is the electric displacement field, $\boldsymbol{B}$ is the magnetic field vector, $\boldsymbol{E}$ is the electric field, $\boldsymbol{H}$ is the magnetic field strength, $\boldsymbol{J}$ is the current density, and ρ is the volume charge density. The term $\partial \boldsymbol{D}/\partial t$ can be also written as $\boldsymbol{J}_{\mathrm{D}}$, as named Maxwell's displacement current. Wang proposed an additional polarization term $\boldsymbol{P}_{\mathrm{S}}$ in the electric displacement field due to the static charge generation in nanogenerator, and thus $\boldsymbol{J}_{\mathrm{D}}$ can be written as:

$$J_{\mathrm{D}} = \frac{\partial \boldsymbol{D}}{\partial t} = \varepsilon \frac{\partial \boldsymbol{E}}{\partial t} + \frac{\partial \boldsymbol{P}_{\mathrm{S}}}{\partial t} \tag{I.2}$$

Therefore, the volume charge density ρ and current density $\boldsymbol{J}$ can be redefined as ρ' and $\boldsymbol{J}'$, respectively:

$$\rho' = \rho - \nabla \cdot \boldsymbol{P}_{\mathrm{S}} \tag{I.3}$$

$$\boldsymbol{J}' = \boldsymbol{J} + \frac{\partial \boldsymbol{P}_{\mathrm{S}}}{\partial t} \tag{I.4}$$

And they still satisfy the charge conversion and continuation equation:

$$\nabla \cdot \boldsymbol{J}' + \frac{\partial \rho'}{\partial t} = 0 \tag{I.5}$$

Through this displacement current as the driving force in nanogenerators, the conduction current can be driven on the external load, forming a complete loop. And then, the output characteristics of TENGs can be further discussed in theoretical models such as Displacement Current Theory model [16, 17], quasi-electrostatic model [18–20], and Distance-Dependent-Electric-Field (DDEF) mode [21–23], which can be used to calculate electric potential and power generation accurately.

I.3 Equivalent Circuit Models and Basic Operation Modes

I.3.1 Equivalent Circuit Models

As stated above, the TENG is operated based on the additional displacement current term, originating from the static charge generated from triboelectric effect. The maintained opposite static charge in triboelectric surfaces determines the inherent capacitive behavior of the TENG. At the open-circuit condition, the potential difference V_{OC} accumulated between electrodes originates from the additional polarization term $\boldsymbol{P}_{\mathrm{S}}$, as a function of the displacement x of the moving part in TENG. In the meanwhile, if we assume no charge generation in TENG, the device can be

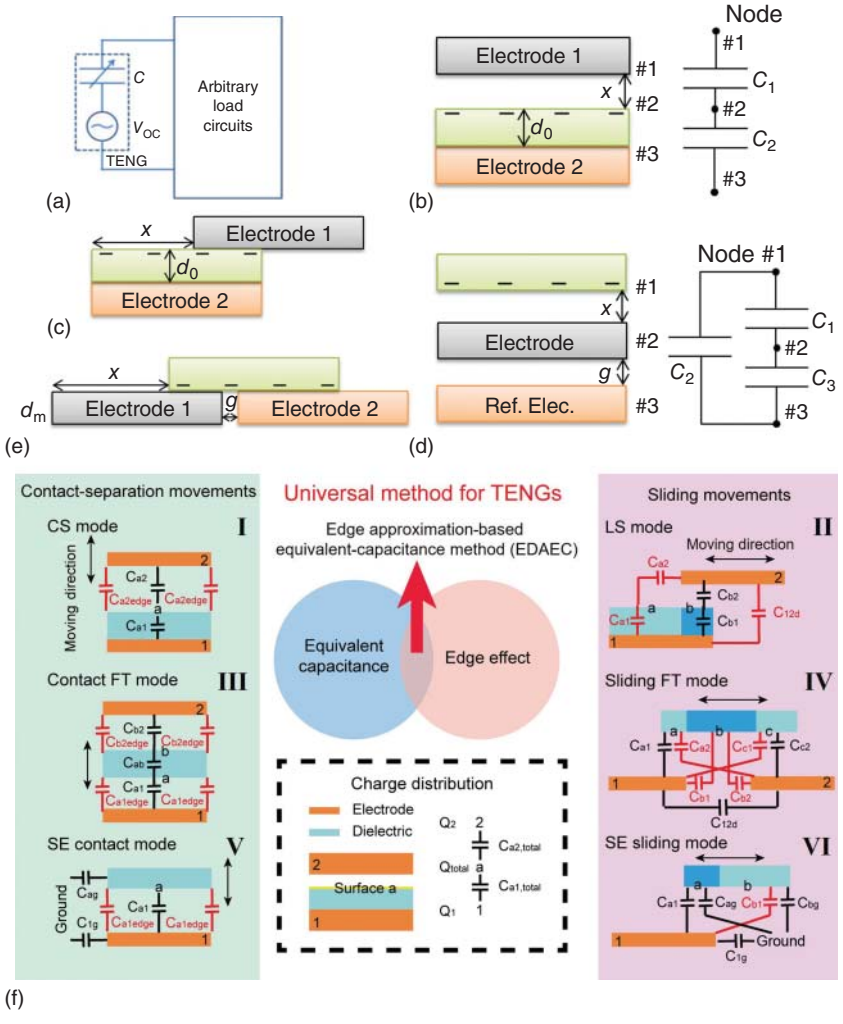

Figure I.1 Equivalent circuit models and basic operation modes of TENGs. (a) Basic equivalent circuit of TENG. Source: Reproduced with permission of [2], 2015 © Elsevier. (b–e) The theoretical models of contact-separation (CS), lateral-sliding (LS), single-electrode (SE), freestanding triboelectric-layer (FT) modes TENGs. (f) The EDAEC method for quantitatively analysis of all modes of TENG. Source: Reproduced with permission of [26], 2019 © Royal Society of Chemistry.

treated as a pure capacitor with capacitance C determined by x as well. So in the generalized case, the output voltage V and the charge transfer Q between electrodes are determined by the equivalent circuit of a voltage source $V_{OC}(x)$ in parallel with a capacitor $C(x)$ as shown in Figure I.1a, with the governing equation described by: [2, 24]

$$V = -\frac{1}{C(x)}Q + V_{OC}(x) \tag{I.6}$$

In short-circuit condition, full charge transfer (Q_{SC}) can be obtained as driven by the voltage source, and hence: [25]

$$Q_{SC}(x) = C(x)V_{OC}(x) \tag{I.7}$$

From such the V-Q-x relationship, we can derive the lumped parameter equivalent circuit mode, which can be used to predict characteristics of TENGs in different modes.

TENG has four basic operation modes: contact-separation (CS), lateral sliding (LS), single electrode (SE), and freestanding triboelectric layer (FT), with detailed structures shown in Figure I.1b–e. In them, SE and FT modes can be further divided into SE contact (SEC), SE sliding (SES), sliding FT (SFT), and contact FT (CFT) modes, depending on whether they are triggered by contact separation or sliding motions. These modes have their own equivalent circuit models available for simulations and theoretical calculations. Here, a universal method for quantitative analysis of all modes of TENG is used for analysis, as shown in Figure I.1f [26]. This method is based on the edge approximation-based equivalent capacitance (EDAEC). The equivalent capacitance models are used to demonstrate charge distributions on each electrode. Due to contact electrification, static triboelectric charges – $Q_{tribo,\chi}$ will be dispersed on the dielectric surface χ after contacting the metal electrodes. According to charge conservation, the metal electrodes would have the same amount of opposite-sign charges in total [27–29]. By defining the charges distributed on electrodes 1 and 2 as Q_1 and Q_2, respectively, the relation can be given below:

$$Q_1 + Q_2 = Q_{tribo} \tag{I.8}$$

Under short-circuit conditions, two electrodes would have the same potential. For simplicity, the two electrodes and the dielectric surface can be defined as node 1, 2 and surface χ (can be different letters for different surfaces), with capacitance between them as $C_{\chi 1,total}$ and $C_{\chi 2,total}$, respectively, as shown in Figure I.1. Therefore, the following equation can be obtained.

$$V_1 = \frac{Q_1}{C_{\chi 1,total}} = V_2 = \frac{Q_2}{C_{\chi 2,total}} \tag{I.9}$$

Thus, the short-circuit equilibrium charges Q_1 and Q_2 on electrodes 1 and 2, respectively, are given as: [30]

$$\begin{cases} Q_1 = \sum \frac{1}{1+\frac{C_{\chi 2,total}}{C_{\chi 1,total}}} Q_{tribo,\chi} \\ Q_2 = \sum \frac{1}{1+\frac{C_{\chi 1,total}}{C_{\chi 2,total}}} Q_{tribo,\chi} \end{cases} \tag{I.10}$$

Sum symbol $\sum$ is used here to indicate the charge contributions from different surfaces. And then:

$$Q_{SC}(x) = |Q_1(x) - Q_1(0)| \tag{I.11}$$

From the equations above, the working mechanism of TENGs can be easily illustrated. When the distance between surface a and electrode 2 is zero the capacitance

across them would be much larger than that across electrode 1 ($C_{\chi 2,\text{total}} \gg C_{\chi 1,\text{total}}$). Most of the positive tribo-charges would be attracted to electrode 2. Q_2 is close to Q_{tribo} and Q_1 is approximately zero. On the other hand, when the distance is quite large, the capacitance across surfaces a and electrode 2 would be much smaller than that across electrode 1 instead ($C_{\chi 1,\text{total}} \gg C_{\chi 2,\text{total}}$). So Q_1 is close to Q_{tribo} and Q_2 is approximately zero. Thus, $Q_{\text{SC}}(x)$ can be calculated by the difference between $Q_1(x)$ and $Q_1(0)$ or between $Q_2(x)$ and $Q_2(0)$, and the total capacitance $C(x) = C_{\chi 1,\text{total}} C_{\chi 2,\text{total}} / (C_{\chi 1,\text{total}} + C_{\chi 2,\text{total}})$. According to this EDAEC method the charge distributed on each electrode could then be quantitatively calculated.

I.3.2 CS Mode TENG

CS mode TENG was the original type TENG demonstrated in early-stage studies [1, 3]. Based on triboelectric materials used, the CS-mode TENG can be divided into two types: dielectric/dielectric contact and dielectric/metal contact. However, since there is no fundamental difference in operation mechanism between these two types, we just take the dielectric/metal contact type as an example, with the model shown in Figure I.1b. The dielectric layer with a thickness of d and relative dielectric constant ε_r is directly facing metal surface as one electrode, and another electrode is attached on the backside of the dielectric layer. Under external excitation, the displacement x is defined as vertical distance between two surfaces. After triboelectric effect, the surface charge density $-\sigma$ was generated in the dielectric surface a with area $S = w \times L$, making $Q_{\text{tribo}} = S\sigma$. By choosing the minimum achievable charge reference state (MACRS) [30], with the charge transfer of Q, the top electrode (electrode 2) is with total charge of $Q_2 = S\sigma - Q$, and the bottom electrode (electrode 1) is with total charge of $Q_2 = Q$. As shown in Figure I.1f-I, the two electrodes and the dielectric layer surface form two capacitances: $C_{\text{a2,total}}(x)$ is the capacitance between electrode 2 and the dielectric surface a, depending on x; and $C_{\text{a1,total}}$ is the capacitance between the dielectric surface a and electrode 1, which is a fixed value which can be considered as parallel-board capacitance. If $S \gg x^2$, the capacitance $C_{\text{a2,total}}(x)$ can be also considered as parallel-board capacitance $C_{\text{a2}}(x)$ without considering the edge effect, and we can derive:

$$Q_{\text{SC}}(x) = \frac{S\sigma x}{d/\varepsilon_r + x} \tag{I.12}$$

$$C(x) = \frac{\varepsilon_0 S}{d/\varepsilon_r + x} \tag{I.13}$$

$$V_{\text{OC}}(x) = \frac{\sigma x}{\varepsilon_0} \tag{I.14}$$

$$V = -\frac{1}{C(x)} Q + V_{\text{OC}}(x) = -\frac{d/\varepsilon_r + x}{\varepsilon_0 S} Q + \frac{\sigma x}{\varepsilon_0} \tag{I.15}$$

While if the edge effect is considered, the total capacitance of $C_{\text{a2,total}}(x)$ should include capacitance contributions from edge effects $C_{\text{a2edge}}(x)$ in parallel, as shown

Figure I.1f-I. Based on previous studies, this capacitance can be estimated as: [31]

$$C_{a2\text{edge}} = \varepsilon_r \varepsilon_0 \left\{ \frac{L}{\pi} \left[1 + \ln\left(1 + 2\pi \frac{w}{\mathrm{d}} + \ln\left(1 + 2\pi \frac{w}{\mathrm{d}} \right) \right) \right] + \frac{\mathrm{w}}{\pi} \left[1 + \ln\left(1 + 2\pi \frac{L}{\mathrm{d}} + \ln\left(1 + 2\pi \frac{L}{\mathrm{d}} \right) \right) \right] \right\} \tag{I.16}$$

With that, we can calculate numerous values for $Q_{\mathrm{SC}}(x)$, $C(x)$, and $V_{\mathrm{OC}}(x)$, obtaining the governing equation.

I.3.3 LS Mode TENG

Traditionally, by assuming the parallel-board capacitance model, the total capacitance $C(x)$ fully depends on the capacitance of the covered part between electrodes 1 and 2, as described in Figures I.1c and I.2a [24, 32, 33]. The length L and the width w of the electrodes and dielectric layers are all defined as 100 mm. The dielectric layer with the thickness of d_0 is stacked on electrode 1 and the gap between the dielectric layer and the sliding electrode 2 is defined as d. The total capacitance $C(x)$, which is based on a traditional unlimitedly large plane, can be described as the equations below:

$$C(x) = \frac{\varepsilon_0 (L - x) w}{d_0/\varepsilon_r + d} \tag{I.17}$$

And the equivalent capacitance of $C(x)$ can also be described as the series connection of $C_{b1}(x)$ and $C_{b2}(x)$, in which:

$$\begin{cases} C_{b1}(x) = \frac{\varepsilon_r \varepsilon_0 (L-x) w}{d_0} \\ C_{b2}(x) = \frac{\varepsilon_0 (L-x) w}{d} \end{cases} \tag{I.18}$$

Here, a new analytical EDAEC model is built, taking the capacitance of edge effect into consideration, to quantitatively describe the TENG's outputs. The real equivalent capacitance of $C(x)$ is shown in Figure I.2b, which includes three parts. Part 1 shows the edge capacitance $C_{a2}(x)$ between the surface a (dielectric layer) and electrode 2, and the capacitance $C_{a1}(x)$ between surface a and electrode 1. $C_{a2}(x)$, which is almost a constant, is quite small when comparing to $C_{a1}(x)$. Therefore $C_{a2(x)}$ can be approximated as a small constant through:

$$\begin{cases} C_{a1}(x) = \frac{\varepsilon_r \varepsilon_0 x w}{d_0} \\ C_{a2}(x) = C_a \end{cases} \tag{I.19}$$

Part 2 in Figure I.2b shows the edge capacitance C_{12d} between electrode 1 and electrode 2, which is also considered as a small constant for easy calculation. And Part 3 shows the capacitance C_{1b2} based on traditional parallel-board capacitance model between the covered part of electrode 1 and electrode 2.

Therefore, the total capacitance $C(x)$ can be calculated as:

$$C(x) = C_{1a2} + C_{12d} + C_{1b2} = \frac{\varepsilon_r \varepsilon_0 x w \cdot C_a}{\varepsilon_r \varepsilon_0 x w + C_a d_0} + C_{12d} + \frac{\varepsilon_r \varepsilon_0 (L - x) w}{\varepsilon_r d + d_0} \tag{I.20}$$

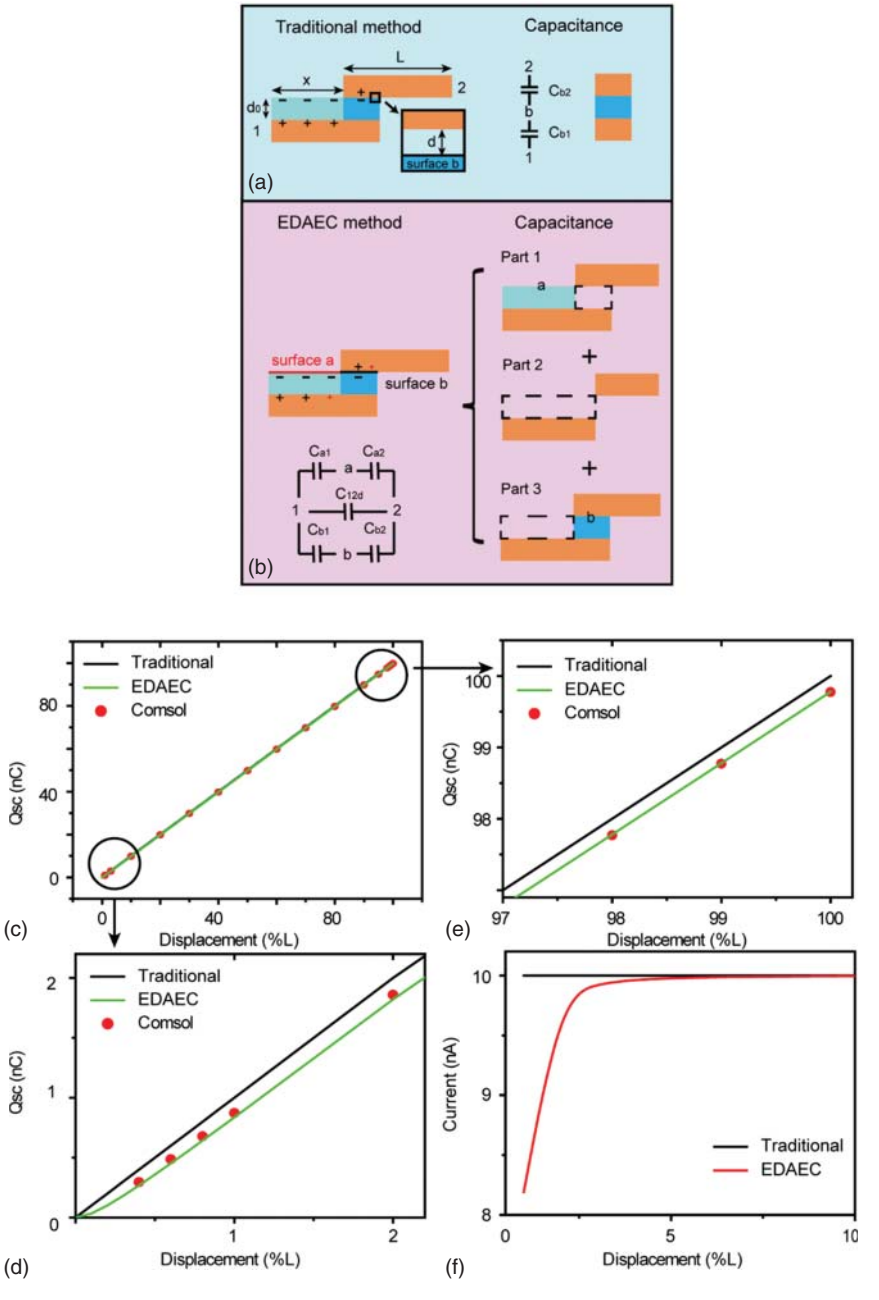

Figure I.2 The traditional mode (a) and the mode of EDAEC method (b) of the LS mode TENG. The comparison of transferred charge by traditional and EDAEC methods (c–e). The comparison of short-circuit current by traditional and EDAEC methods. Source: Reproduced with permission of [26], 2019 © Royal Society of Chemistry.

With triboelectric charge density σ, total triboelectric charge on surface sections a and b can be defined as the equations below:

$$\begin{cases} Q_a = \sigma w(x) \\ Q_b = \sigma w(L-x) \end{cases} \tag{I.21}$$

Under the short-circuit (SC) condition, electrode 1 and electrode 2 will have the same electrical potential. Therefore, the total charges on each electrode can be derived from Equation (I.10) by overlapping electrostatically induced charges from Q_a and Q_b:

$$\begin{cases} q_{a1}(x) = \frac{C_{a1}}{C_{a1}+C_{a2}} Q_a = \frac{\varepsilon_r \varepsilon_0 xw}{\varepsilon_r \varepsilon_0 xw + d_0 C_a} \sigma wx \\ q_{a2}(x) = \frac{C_{a2}}{C_{a1}+C_{a2}} Q_a = \frac{d_0 C_a}{\varepsilon_r \varepsilon_0 xw + d_0 C_a} \sigma wx \\ q_{b1}(x) = \frac{C_{b1}}{C_{b1}+C_{b2}} Q_b = \frac{\varepsilon_r d}{\varepsilon_r d + d_0} \sigma w(L-x) \\ q_{b2}(x) = \frac{C_{b1}}{C_{b1}+C_{b2}} Q_b = \frac{d_0}{\varepsilon_r d + d_0} \sigma w(L-x) \end{cases} \tag{I.22}$$

Therefore, the total charges on electrode 1 Q_1 can be calculated as:

$$\begin{aligned} Q_1(x) &= q_{a1} + q_{b1} = \frac{\varepsilon_r \varepsilon_0 xw}{\varepsilon_r \varepsilon_0 xw + d_0 C_a} \sigma wx + \frac{\varepsilon_r d}{\varepsilon_r d + d_0} \sigma w(L-x) \\ &= \left(\sigma w \frac{d_0}{\varepsilon_r d + d_0} \right) x + \frac{\left(\frac{d_0 C_a}{\varepsilon_r \varepsilon_0 w} \right)^2 \sigma w}{x + \frac{d_0 C_a}{\varepsilon_r \varepsilon_0 w}} + \sigma wL \frac{\varepsilon_r d}{\varepsilon_r d + d_0} - \sigma \frac{d_0 C_a}{\varepsilon_r \varepsilon_0} \end{aligned} \tag{I.23}$$

When $x = 0$ is assigned to be the initial state, the initial Q_1 is defined as:

$$Q_1(0) = \sigma wL \frac{\varepsilon_r d}{\varepsilon_r d + d_0} \tag{I.24}$$

The transferred charges Q_{SC} is equal to the change of the charge on electrode 1, therefore the transferred charge Q_{SC} can be calculated as the difference between the induced charges $Q_1(x)$ and the initial state charges $Q_1(0)$ on electrode 1. The short-circuit charge Q_{SC} can be calculated by the equation below.

$$Q_{SC}(x) = |Q_1(x) - Q_1(0)| = \left(\sigma w \frac{d_0}{\varepsilon_r d + d_0} \right) x + \frac{{Z_a}^2 \sigma w}{x + Z_a} - \sigma w Z_a \tag{I.25}$$

In the equation above, Z_a is a constant when the structure is fixed:

$$Z_a = \frac{C_a d_0}{\varepsilon_r \varepsilon_0 w} \tag{I.26}$$

It should be noticed that the first item of Q_{SC} has a linear relationship with displacement x, representing the part of σwx from traditional method. The second item of Q_{SC} is a non-linear item, and the third item is a constant.

Traditionally, the graph of traditional Q_{SC} has a strictly linear relationship with x. However, in the new EDAEC method, as we consider the edge effect, the Q_{SC} does not have a strictly linear relationship with the displacement. As shown in Figure I.2c, the graph of Q_{SC} has a flatter start at the beginning (Figure I.2d), and then the slope of Q_{SC} will increase until it has almost the same slope with the traditional graph when

$d = 0$ (Figure I.2e). In order to validate the above theoretical derivation, an LS mode TENG model is simulated by finite element method (by COMSOL Multiphysics software package), and the corresponding results are plotted in Figure I.2c–e. It should be emphasized that the theoretically calculated Q_{SC} by COMSOL simulation is closer to that from our EDAEC model than traditional Q_{SC}. According to the results of Q_{SC}, the graph of current and displacement is also plotted with a constant sliding speed of 0.01 m/s. Unlike the traditional graph which gives constant current, the EDAEC method shows that the current would be much lower when x is small and then sharply increase to the traditional value (in Figure I.2f). These results demonstrate that our EDAEC model which considers the edge effect is more suitable when describing the LS mode TENG.

With the total capacitance $C(x)$ and the short-circuit charge Q_{SC} known, the open-circuit voltage can be obtained. The capacitance calculated by the EDAEC method is demonstrated to be more accurate than traditional values (Figure I.3a) as compared to the COMSOL results. The open-circuit voltages are also plotted in Figure I.3b, which gradually increase with displacement x, and increase sharply when x is quite close to L. The total capacitance of the LS TENG will be zero according to the traditional method at $x = L$. At this position, the open-circuit voltage will be infinitely large, which is far away from the real situation. The EDAEC method takes the edge capacitance into consideration, and thus the open-circuit voltage can be accurately calculated even when $x = L$. Compared to traditional calculation, the EDAEC method shows that the voltage will give a result which is more consistent with that by COMSOL, as shown in Figure I.3b.

According to Equation (I.24), the transferred charge Q_{SC} is also affected by the TENG's structural parameters, for example, the distance d between the dielectric material and electrode 2, and the thickness d_0 of the dielectric material. Therefore, the short-circuit transferred charges and open-circuit voltages with different gap d is also demonstrated in Figure I.3c,d. It is obvious that the slopes of Q_{SC} and V_{OC} against the change of x become much smaller when the gap d increases. This result can explain experimental phenomenon of why the outputs (Q_{SC} and V_{OC}) of the LS TENG become quite low when the gap between the dielectric material and electrode 2 is larger than a threshold value. The thickness d_0 of the dielectric material will also affect the LS TENG's outputs, as shown in Figure I.3e,f. The Q_{SC} against x will become a bit smaller when the dielectric thickness d_0 increases, while the V_{OC} will become much larger due to the decrease in the total capacitance. These results are also compared with the simulation results by COMSOL, which shows a high degree of agreement. Based on the above analysis, the EDAEC method, by considering the edge effect, shows high accuracy in calculating the capacitance $C(x)$, short-circuit charge Q_{SC} and open-circuit voltage V_{OC} of LS mode TENGs under different conditions. It should be emphasized that this EDAED method is quite important for the grating structured TENGs. Because the electrode sizes of the grating structured TENGs are much smaller than other sliding TENGs, the electrodes could not be regarded as the traditional unlimitedly large plane anymore. Therefore, the influence of the side-effect capacitance will become much more

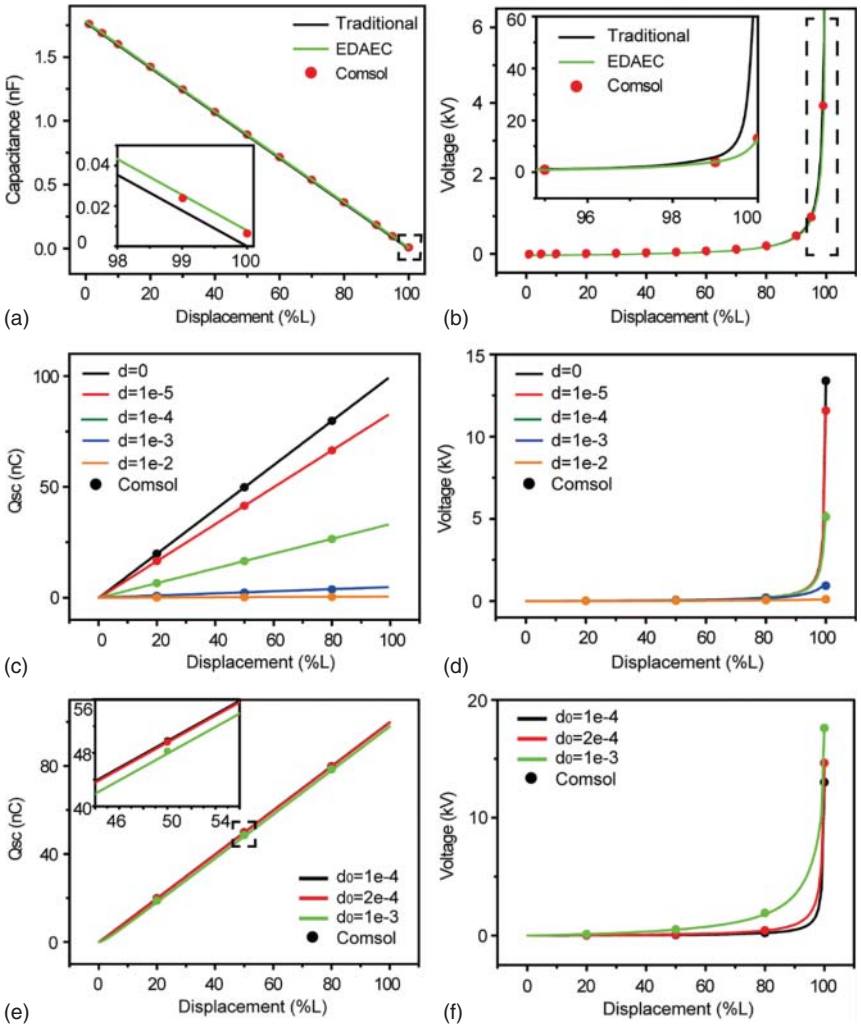

Figure I.3 Comparison of traditional and the EDAEC method on capacitance (a) and voltage (b). The insets are the magnified graph of the dotted part. (c) The relationship between transferred charges at short-circuit and the separation distance *d*. (d) The relationship between open-circuit voltage and the separation distance *d*. (e) The relationship between transferred charges at short-circuit and the thickness of dielectric layer d_0. (e) The relationship between open-circuit voltage and the thickness of dielectric layer d_0. Source: Reproduced with permission of [26], 2019 © Royal Society of Chemistry.

significant. The short-circuit charge of the grating structured TENGs is no longer a straight line [34].

I.3.4 SE Mode TENG

SE mode TENG is a design that utilizes only one electrode to collect output and connect to the external device, getting rid of the moving electrode which may bring

limitations in applications. However, in practical applications, the other connection node of the external devices is always connected to the ground, so the ground should be considered as a reference electrode for SE-TENGs. Here we will introduce models for SEC and SES modes TENGs.

(1) SEC mode TENG

We take the conduct-to-dielectric SEC TENG as an example, with the structure shown in Figure I.1d. The output of dielectric-to-dielectric SEC TENG will be slightly different, but they follow similar characteristics. The top dielectric serves as the moving part, with the bottom surface a taking charge density of -σ, and the surface area of $S = w \times L$, making $Q_{\text{tribo}} = S\sigma$. The electrodes in TENG and the ground are marked as nodes "1" and "2", respectively. The gap between the electrode and the ground is g, while the displacement of the dielectric is x which is defined as the gap between the dielectric bottom surface a and the electrode. By choosing the minimum achievable charge reference state (MACRS), with the charge transfer of Q, the electrode is with total charge of $Q_1 = S\sigma - Q$, and the ground is with total charge of $Q_2 = Q$. As shown in Figure I.1f-V, the electrode, dielectric surface a, and reference electrode forms 2 capacitances: C_{a1} is the capacitance between the electrode and the dielectric surface a, depending on x, which is infinite at $x = 0$; C_{a2} is the capacitance between the ground and the dielectric surface a, depending on x. In this mode, the direct capacitance C_3 between the electrode and ground should also be considered, except the short-circuit condition [25]. The actual capacitance between the electrode and ground can be obtained by considering the connections among the three capacitances:

$$C(x) = C_3 + \frac{C_{\text{a1}} C_{\text{a2}}}{C_{\text{a1}} + C_{\text{a2}}} \tag{I.27}$$

Therefore, according to Eqs. I.7, I.10, and I.11, the short-circuit charge can obtained as:

$$Q_{\text{SC}}(x) = |Q_1(x) - Q_1(0)| = \left| \frac{\sigma S}{1 + \frac{C_{\text{a2}}}{C_{\text{a1}}}} - \frac{\sigma S}{1 + \frac{C_{\text{a2}}(0)}{C_{\text{a1}}(0)}} \right| = \sigma S \frac{C_{\text{a2}}}{C_{\text{a1}} + C_{\text{a2}}} \tag{I.28}$$

$$V_{\text{OC}}(x) = \frac{Q_{\text{SC}}(x)}{C(x)} = \frac{\sigma S C_{\text{a2}}}{C_{\text{a1}} C_{\text{a2}} + C_{\text{a1}} C_3 + C_{\text{a2}} C_3} \tag{I.29}$$

Please note that in SEC TENG, if we use the parallel-board capacitance for these capacitances, there will be no output, since the edge effects play an important role in SEC TENG. We can use Equation (I.16) to calculate these capacitances, obtaining numerous values for $Q_{\text{SC}}(x)$, $C(x)$, and $V_{\text{OC}}(x)$, and the governing equation.

(2) SES mode TENG

Owing to only one electrode, it is difficult for researchers to quantitatively describe output performances of the SES TENG [25]. The EDAEC method mentioned above can solve this problem. The mode in Figure I.4a is designed to demonstrate the working principle of the SES TENG, as the ground could be regarded as the second

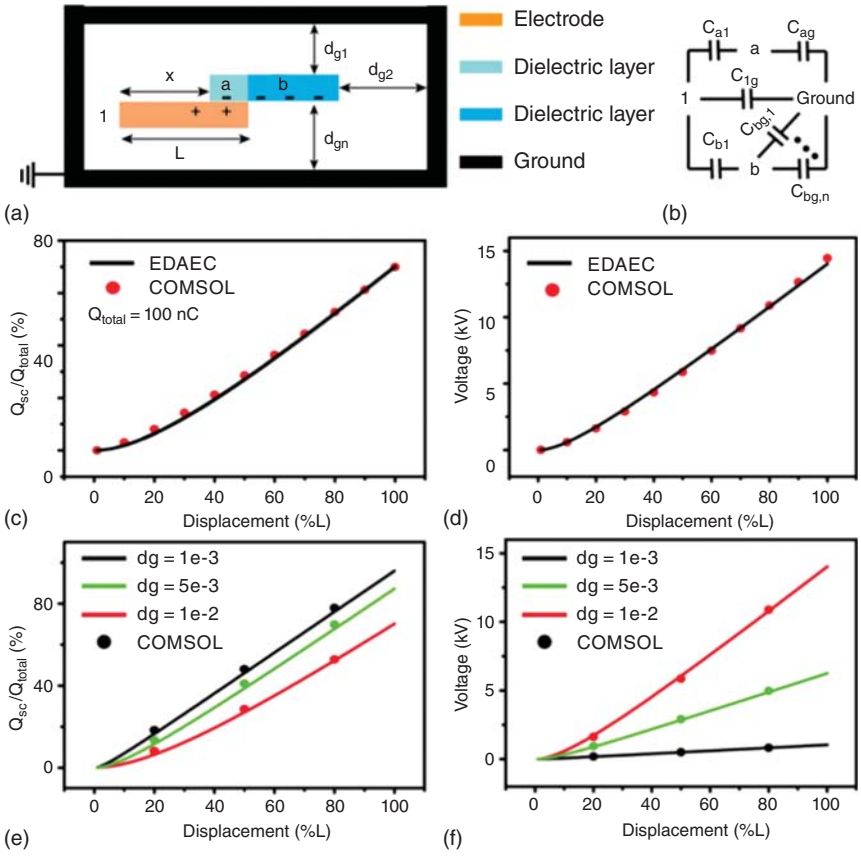

Figure I.4 The schematic (a) and equivalent capacitance (b) of SES TENG. (c) The relationship of transferred charges with the displacement. (d) The relationship of open-circuit voltage with the displacement. (e,f) The relationship between transferred charges at short-circuit (e) and open-circuit voltage (f) with the distance between the dielectric layer and the ground d_g. Source: Reproduced with permission of [26], 2019 © Royal Society of Chemistry.

electrode of the single-electrode TENG. Similar to the method described before, the metal electrode 1 and the dielectric layer are defined with length $L = 100\,\text{mm}$ and width $w = 100\,\text{mm}$. The distance between dielectric layer and electrode 1 is defined as d, and the distance between the dielectric layer and the ground is defined as d_g. The surrounding environment connected to the ground will have an effect to the d_g, which could be regarded as a big conductive box containing the SES TENG.

The equivalent capacitance of C_{total} is shown in Figure I.4b, which includes three parts, including the capacitances between electrode 1 and the ground electrode *via* surfaces a (C_{a1} and C_{ag}), and b (C_{b1} and C_{bg}). Because the ground electrode is surrounding the dielectric layer, therefore there are several in-parallel capacitances $C_{bg,n}$ between the dielectric layer and each surrounding surface, and C_{bg} is the total

capacitance. And C_{1gd} is the direct capacitance between electrode 1 and the ground electrode. The capacitance can be defined by the following equations.

$$\begin{cases} C_{a1(x)} = \frac{\varepsilon_0 w(L-x)}{\mathrm{d}} \\ C_{ag(x)} = \frac{\varepsilon_0 w(L-x)}{\mathrm{dg}} \\ C_{bg(x)} = \frac{\varepsilon_0 w(x)}{\mathrm{dg}} \\ \frac{1}{d_g} = \sum_{i=1}^{n} \frac{1}{d_{g_i}} \end{cases} \tag{I.30}$$

According to the EDAEC we described before, the edge capacitance C_{b1} is quite small as compared with other capacitances. Therefore, C_{b1} can be approximated as a small constant. The total capacitance could be defined as:

$$C_{\text{total}} = C_{1ag} + C_{1gd} + C_{1bg} = \frac{C_{a1} * C_{ag}}{C_{a1} + C_{ag}} + C_{1gd} + \frac{C_{b1} * C_{bg}}{C_{b1} + C_{bg}} \tag{I.31}$$

After contact electrification, the upper surface of the dielectric layer would be filled with triboelectric charges. Under short-circuit conditions, the total charges on electrode 1 can be calculated by the following equations.

$$\begin{aligned} Q_1(x) &= q_{a1} + q_{b1} = \frac{1}{1 + \frac{C_{ag}}{C_{a1}}} Q_a + \frac{1}{1 + \frac{C_{bg}}{C_{b1}}} Q_b \\ &= \left(\frac{d_g}{d_g + d} \right) \sigma w(L - x) + Z\sigma w \left(1 - \frac{z}{Z + x} \right) \end{aligned} \tag{I.32}$$

In the equation above, to facilitate the calculation, the constant is defined as:

$$Z = \frac{C_{b1} d_g}{w\varepsilon_0} \tag{I.33}$$

Thus, the short-circuit charge Q_{SC} can be calculated by the equation below.

$$Q_{\text{SC}}(x) = |q_1(0) - q_1(x)| = \left(\frac{d}{d_g + d} \right) \sigma w x + z^2 \sigma w \frac{1}{Z + x} - Z\sigma w \tag{I.34}$$

Due to the characteristics of the single electrode TENGs, the short-circuit charge Q_{SC} is noticeably lower than the total charges on the electrode 1 Q_{total}, which is equal to the total triboelectric charge of the dielectric layer. From Figure I.4c, at $x = L$, the short-circuit charge Q_{SC} only reaches around 70% of the total movable charge Q_{total}. This phenomenon could explain why the output power or the efficiency of SE TENG is quite lower than LS or SFT TENG. To validate the above equations, a SES TENG model is simulated by COMSOL. The transferred charge from the equation and the numerical results simulated from COMSOL are plotted in Figure I.4c which are quite consistent with our model.

With the total capacitance C_{total} and the short-circuit charge Q_{SC} known, the open-circuit voltage can be obtained by Equation (I.7). The open-circuit voltage from the equation and the results simulated from COMSOL are plotted on the same graph to compare, in Figure I.4d. The theoretical calculation coincides with

numerical simulation, which demonstrates the accuracy of the proposed theoretical model.

According to Equation (I.34), the distance d_g between the dielectric material and the ground electrode will significantly affect the transferred charge Q_{SC}. Therefore, the transferred charge and open-circuit voltage with different distance d_g is also demonstrated in Figure I.4e,f. It is interesting to notice that the slope of Q_{SC} will be much smaller when the distance d_g increases, while V_{OC} will be much larger.

I.3.5 FT Mode TENG

FT TENG is another two-electrode TENG design that can make both electrodes keep static, while the high output performance can be guaranteed [30]. It can also be distinguished from CFT and SFT modes.

(1) CFT mode TENG

The CFT can also be divided by the different material selections as dielectrics or conductors, while their output characteristics are quite similar. Here, we just introduce a typical one with the dielectric freestanding layer and metal electrodes, as shown in Figure I.1f-III. The dielectric freestanding layer serves as the moving part, with the top and bottom surfaces a and b taking charge density of $-\sigma$ for each, and the surface area of $S = w \times L$, making $Q_{\text{tribo,a}} = Q_{\text{tribo,b}} = S\sigma$. The top and bottom metal electrodes are marked as nodes "1" and "2", respectively. The gap between the electrodes is g, while the displacement of the dielectric layer is x, which is defined as the distance between the bottom dielectric surface b and the bottom electrode 2. The dielectric thickness is d with relative dielectric constant ε_r. As shown in Figure I.1f-III, the electrodes 1, 2, and dielectric surfaces a, b can form 3 capacitances: C_{a1} is the capacitance between the top electrode 1 and the dielectric surface a, depending on $g-x$, which is infinite at $x = g$; C_{ab} is the capacitance of the dielectric layer, which is a constant estimated by the parallel-board capacitance; C_{b2} is the capacitance between the electrode 2 and the dielectric surface b, depending on x, which is infinite at $x = 0$.

Q_1 and Q_2 of this CFT TENG can be derived as the sum of charge contributed from two charged surfaces a and b, and then:

$$\begin{cases} Q_1 = \frac{1}{1+\frac{C_{a2,\text{total}}}{C_{a1,\text{total}}}} Q_{\text{tribo},a} + \frac{1}{1+\frac{C_{b2,\text{total}}}{C_{b1,\text{total}}}} Q_{\text{tribo},b} = \sigma S \frac{\frac{1}{C_{ab}}+\frac{2}{C_{b2}}}{\frac{1}{C_{a1}}+\frac{1}{C_{ab}}+\frac{1}{C_{b2}}} \\ Q_2 = \frac{1}{1+\frac{C_{a1,\text{total}}}{C_{a2,\text{total}}}} Q_{\text{tribo},a} + \frac{1}{1+\frac{C_{b1,\text{total}}}{C_{b2,\text{total}}}} Q_{\text{tribo},b} = \sigma S \frac{\frac{1}{C_{ab}}+\frac{2}{C_{a1}}}{\frac{1}{C_{a1}}+\frac{1}{C_{ab}}+\frac{1}{C_{b2}}} \end{cases} \tag{I.35}$$

And then:

$$Q_{SC}(x) = |Q_1(x) - Q_1(0)| = \sigma S \left(\frac{\frac{1}{C_{ab}} + \frac{2}{C_{b2}}}{\frac{1}{C_{a1}} + \frac{1}{C_{ab}} + \frac{1}{C_{b2}}} - \frac{C_{a1}(0)}{C_{a1}(0) + C_{ab}} \right) \tag{I.36}$$

$$C(x) = C_{a1} \| C_{ab} \| C_{b2} \tag{I.37}$$

So $V_{OC}(x)$ can be also calculated correspondingly. If $S \gg g^2$, the capacitance $C_{a1}(x)$ and $C_{b2}(x)$ can be also considered as parallel-board capacitances without considering

the edge effect, and we can derive:

$$Q_{SC}(x) = \frac{2S\sigma x}{d/\varepsilon_r + g} \tag{I.38}$$

$$C(x) = \frac{\varepsilon_0 S}{d/\varepsilon_r + g} \tag{I.39}$$

$$V_{OC}(x) = \frac{2\sigma x}{\varepsilon_0} \tag{I.40}$$

$$V = -\frac{1}{C(x)}Q + V_{OC}(x) = -\frac{d/\varepsilon_r + g}{\varepsilon_0 S}Q + \frac{2\sigma x}{\varepsilon_0} \tag{I.41}$$

If the edge effect is considered, the total capacitance of these two capacitors should include capacitance contributions from edge effects in parallel, as shown in Figure I.1f-III. Based on previous studies, this capacitance can be estimated by Equation (I.16). With that, we can calculate numerous values for $Q_{SC}(x)$, $C(x)$, and $V_{OC}(x)$, obtaining the governing equation.

(2) SFT mode TENG

The capacitance caused by edge effect in sliding FT (SFT) TENG is significant and brings a much more obvious influence than that for LS TENG. The simplest structure of the SFT TENG, shown in Figure I.1e, consists of two adjacent metal electrodes (length: $L = 100$ mm, width: $w = 100$ mm) with a gap g and a movable dielectric layer with identical size to each electrode. The dielectric layer is placed above the electrodes at a distance of d. Due to impact of the edge capacitance, the sliding displacement of the TENG can be divided into three sections according to x, $0 < x < g$ (Part 1, Figure I.5a,b), $g \le x \le L$ (Part 2, Figure I.5c,d), and $L < x < L + g$ (Part 3), which is symmetric to Part 1. Therefore, both the short-circuit transferred charge Q_{SC} (Figure I.5e,f) and open-circuit voltage (Figure I.5g,h) can be divided into 3 parts correspondingly: the first flat part corresponding to $0 < x < g$, the second linear-like part corresponding to $g \le x \le L$ and the third flat part corresponding to $L < x < L + g$.

When $g \le x \le L$, the total capacitance (Figure I.5c) consists of the capacitances between electrodes *via* surfaces a (C_{a1} and C_{a2}), b (C_{b1} and C_{b2}), and c (C_{c1} and C_{c2}), and the direct capacitance between electrodes (C_{12d}). Traditionally, only C_{a1} and C_{c2} are considered, which can be given by the following equations.

$$\begin{cases} C_{a1(x)} = \frac{\varepsilon_0 w(L-x)}{d} \\ C_{c2(x)} = \frac{\varepsilon_0 w(x-g)}{d} \end{cases} \tag{I.42}$$

Similar to the Equation (I.19) of LS TENG, C_{a2} and C_{c1} are quite small, which can be approximated as small constants. Due to the structural symmetry, C_{b1} is equal to C_{b2}, thus $Y_b = C_{b2}/C_{b1} = 1$. Therefore, according to the charge distribution Equation (I.10), the charge distributed on the electrode 1 can be defined as:

$$Q_1(x) = q_{a1} + q_{b1} + q_{c1} = \frac{1}{1 + \frac{C_{a2}}{C_{a1}}}Q_a + \frac{1}{1 + \frac{C_{b2}}{C_{b1}}}Q_b + \frac{1}{1 + \frac{C_{c2}}{C_{c1}}}Q_c \cdot (g \le x \le L) \tag{I.43}$$

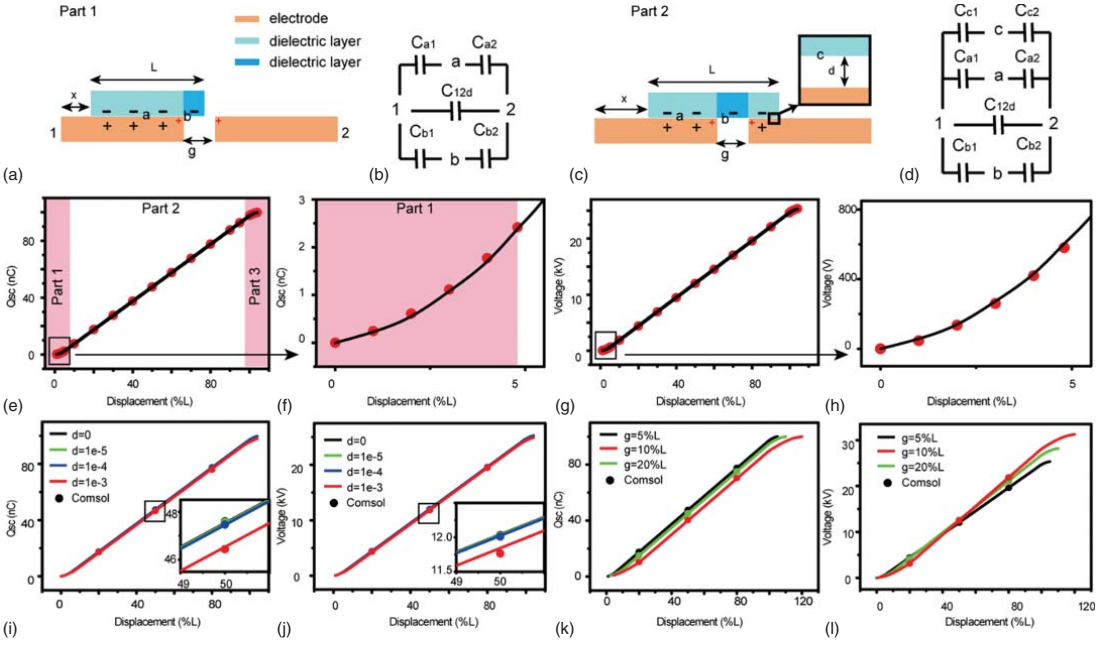

Figure I.5 The schematic (a) and equivalent capacitance (b) of SFT TENG part 1. The schematic (c) and equivalent capacitance (d) of SFT TENG part 2. (e) The total transferred charges of three parts with the displacement. (f)The magnified graph of the dotted part 1 of (e). (g) The total open-circuit voltage of three parts with the displacement. (h) The magnified graph of the dotted part 1 of (g). (i,j) The relationship between transferred charges at short-circuit (i) and open-circuit voltage (j) with the separation distance *d*. (k,l) The relationship between transferred charges at short-circuit (k) and open-circuit voltage (l) with the gap *g*. Source: Reproduced with permission of [26], 2019 © Royal Society of Chemistry.